



Heterogeneous Deformable Modeling and Topology Modification for Surgical Cutting Simulation with Haptic Interfaces

Shiyong Lin¹, Roger Narayan² and Yuan-Shin Lee³

¹North Carolina State University, slin@ncsu.edu

²University of North Carolina at Chapel Hill, roger_narayan@msn.com

³North Carolina State University, yslee@ncsu.edu

ABSTRACT

In this paper we propose methodology and algorithms to generate realistic cuts on heterogeneous deformable object models. A 3-dimensional node snapping algorithm is presented to modify the topology of deformable models, without adding new elements. Smooth cut is generated by duplicating and displacing mass points that have been snapped along the cutting path. Several sets of triangles representing different soft tissues are generated along the new cut to present the internal structures and material properties of heterogeneous deformable objects. A haptic device is integrated into cutting simulation system as a cutting tool. The proposed cutting techniques can be used in surgical simulation or other virtual simulations involving topological modification of heterogeneous soft materials to enhance the fidelity and realism.

Keywords: medical cutting simulation, heterogeneous deformable modeling, haptic interface.

DOI: 10.3722/cadaps.2008.877-888

1. INTRODUCTION

Medical surgical simulation is a technology dedicated to medical training and surgery planning. Cutting simulation is the key component and also the most difficult one in surgical simulators. Cutting is a common operation in both conventional and minimal invasive surgeries. Most surgical tasks begin with an incision to expose the surgical region. However, it is a difficult task to simulate cutting operation since the topology of deformable models is changing in real-time and a large amount of computation is required. Cutting in real surgery is a careful step-by-step procedure to reach desirable cutting depth. The cutting tool is very often perpendicular to the target surface. Each movement of cutting tool is relatively simple, often short and straight [1]. Soft tissues are typically not cut too deep at once for the sake of avoiding unnecessary damage to internal healthy tissues. For example, in the middle line laparotomy, surgical incision routine begins with skin incision, followed by subcutaneous layer incision and peritoneum incision [2]. It is very important to show realistic internal structures at the cutting site as the visual clue, especially for surgical training and planning purposes.

In most of the current cutting simulations, cutting operation is considered only with surface models or homogeneous volumetric models [3-5]. In general, it is relatively easy to modify the topology of surface based models since only surface meshes are involved in cutting. Groove or gutter is often created along the cutting path to give the realistic illusion of volumetric cut [6-7]. Surface based models are not suitable for most soft tissues like muscles, especially when internal structures or material properties of these models play a critical role in the cutting procedure.

On the other hand, cutting simulation on volumetric deformable models is normally implemented by three types of topological modification approaches, e.g. element removal, mesh subdivision, and mesh adaptation. Element removal

is directly to remove an element intersecting with the tool [9]. Despite of its simplicity and computational efficiency, this method cannot present smooth cut because of visual artifacts. Mesh subdivision can generate smooth cutting path by subdividing tetrahedrons [5] along the cutting planes. However, the method is computationally expensive due to many subdivision cases and increasing element number. Another drawback is that smaller or degenerated elements may be created near the cutting site, which can cause instability of the simulation [5]. Mesh adaptation (or node snapping) shown can generate good cutting path without creating new elements. Mass points near cutting path are snapped to the closest points on the cutting path such that some related edges (or springs) are aligned along the cutting path. Mesh adaptation was applied in tetrahedral mesh [8]. In our previous work, heterogeneous deformable object modeling technique has been proposed to model heterogeneous soft tissues [10-11]. The quality of resulting incision is limited by initial mesh resolution. The smaller size of elements, the smoother cut can be accomplished by node snapping. However, current cutting approaches only deal with homogeneous tetrahedral models. Soft tissue layers around the cutting site couldn't be presented as often observed in real surgery.

In this paper, a 3D cutting method is proposed to simulate the medical cutting operation on heterogeneous deformable models. Technique of constructing heterogeneous deformable models is presented for modeling heterogeneous biological soft tissues. To simulate surgical cutting, a 3D topological modification method is presented for cutting simulation on heterogeneous deformable models. The presented techniques can be used for medical surgical simulation and deformable objects modeling.

2. HETEROGENEOUS DEFORMABLE OBJECT MODELING

Biological soft tissues are viscoelastic, anisotropic and heterogeneous deformable objects [12]. As shown in Figure 1, a heterogeneous deformable object may include various soft and hard materials. For example, human legs consist of skin, fat tissue, various muscles, bones and other soft tissues. It is of great importance to model biological soft tissues heterogeneously in order to simulate realistic surgical procedures [10]. We have proposed a tri-ray node snapping algorithm to generate heterogeneous deformable models from boundary or interface surfaces of biological soft tissues [13]. Fig. 1 shows the boundary surfaces of skin, bones, and various muscles in a human leg and also the heterogeneous human leg model generated from these boundary surfaces.

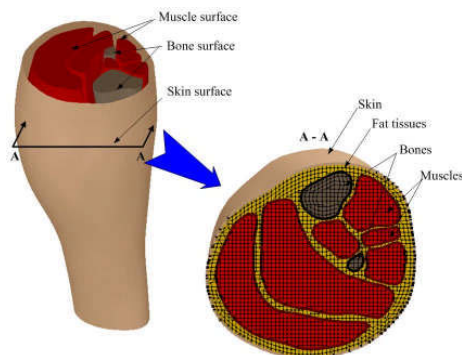


Fig. 1: Heterogeneous soft tissue model.

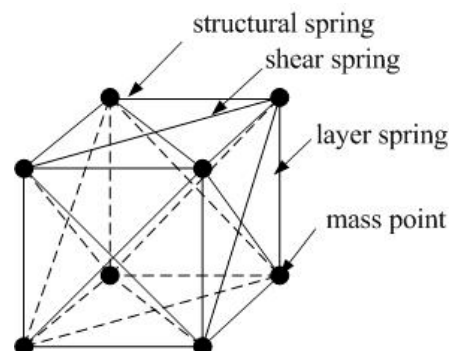


Fig. 2: Hexahedral volumetric Mass Spring model.

Deformable object model generation is a process of discretizing volumetric objects into mass points and springs in Mass Spring Model or small elements in Finite Element Model [14-15]. In our previous work in [13], heterogeneous deformable models of biological soft tissues have been generated based on volumetric Mass Spring Model. The heterogeneous deformable model consists of hexahedral mass spring elements, as shown in Fig. 2. Mass points on the same layer are connected by structural springs and diagonal shear springs as shown in Fig. 2. Structural springs stand for tensile and compressive stress, while shear springs are used for shear stress. Layer springs are added to connect neighboring tissue layers. One soft tissue may consist of several mass spring layers depending on its thickness. For simplicity, many examples shown in this paper doesn't show the structural springs.

3. SUGICAL CUTTING ON HETEROGENEOUS MODELS

In this paper, we present the 3D node snapping and topological modification techniques to simulate the surgical cutting operation on heterogeneous deformable models. Hexahedral mass spring structure is maintained without

producing extra elements during the topological modification. The main objective of the algorithm is to generate heterogeneous soft tissue layers at the cutting site. For the discussion of the proposed algorithm, some definitions are first given as followings:

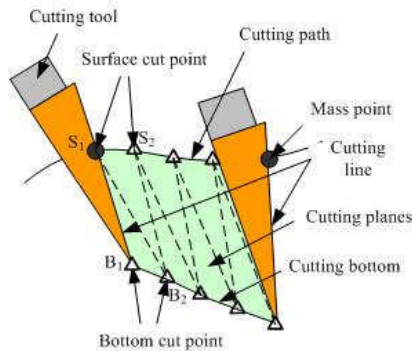


Fig. 3: Definitions for volumetric deformable object cutting.

Surface cut points: if the cutting tool cuts into a deformable model, it intersects the model surface at the surface cut points (e.g. S_1 and S_2 in Fig. 3).

Bottom cut points: tips of the cutting tool are defined as the bottom cut points (e.g. B_1 and B_2), when the cutting tool cuts into a model.

Cutting lines: line segments between a pair of a surface cut point and a bottom cut point such as S_1B_1 and S_2B_2 are defined as the cutting lines. Vectors $\overrightarrow{S_iB_i}$ are cutting tool orientations.

Cutting path: the cutting path consists of line segments connecting the surface cut points on the model surface.

Cutting bottom: the cutting bottom consists of line segments connecting the bottom cut points inside the deformable model.

Cutting planes: movements of the cutting tool are represented by a series of cutting planes. There are two triangles formed by two cutting lines if the two cutting lines are not parallel. For example, two planes represented by triangle $S_1S_2B_2$ and $S_1B_1B_2$ exist between cutting lines S_1B_1 and S_2B_2 . Since the cutting tool is often manipulated approximately perpendicular to the model surface, the two triangles are approximately parallel. In this paper, the triangle including two surface cut points such as triangle $S_1S_2B_2$ is used to approximate the cutting plane between two cutting lines.

The cutting algorithm is implemented in the following four phases: (i) surface cut snapping, (ii) inside cut snapping, (iii) cut open generation, (iv) internal triangle generation. Details of the algorithm are explained in the following sections.

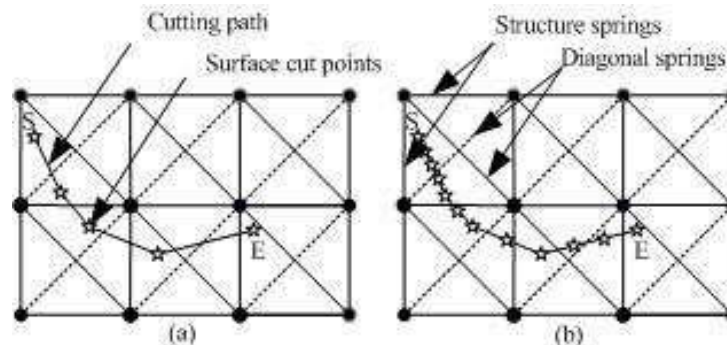


Fig. 4: Surface cut points sampling at different cutting speed and intersection points.

3.1 Surface Cut Node Snapping

In this step, mass points close to the cutting path are snapped along the cutting path on the deformable object surface. In the snapping approach, some springs are aligned along the cutting path, which are used to generate the cut

opening. First, surface cut points are sampled when the cutting tool intersects the model surface. The slower the cutting tool moves, the more surface cut points can be recorded. For example, more surface cut points are obtained at slower cutting speed in Fig. 4(b) than those obtained at higher cutting speed in Fig. 4(a). Intersection points between the cutting path and springs on the model surface are then calculated as shown in Fig. 5(a). Intersection points are dependent not on the cutting speed but on the cutting path. For each intersection point, the closest mass point is snapped to the intersection point. As a result, some springs are displaced along the cutting path. The snapping and cutting is a progressive process. Before the cutting tool intersects a spring, the last cutting tool position should be updated as the temporary cutting end point. And the cut will be generated and temporarily ends here. This is especially important for visual realism when the cutting tool moves very slowly and the cut should still be updated in the real time.

In this method, only structural springs are used to calculate intersection points due to following two reasons. First, fewer springs are used for intersection testing to reduce the computational burden. More importantly, intersection with diagonal springs may result in degeneracy that all three vertexes of a triangle are snapped into the cutting line. For example, triangles abc and abd are snapped to the cutting path and both triangles disappear as shown in Fig. 5(b). Degeneracy can cause the instability of deformable object simulation [13]. On the contrary, such degeneracy can be eliminated by allowing only structural springs for intersection, as shown in Fig. 5(c).

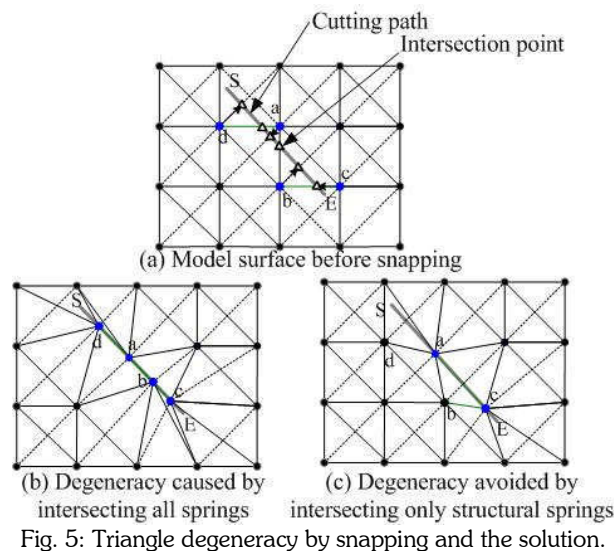


Fig. 5: Triangle degeneracy by snapping and the solution.

During the surface cut snapping, a mass point is possibly the closest point to several intersection points. For instance, mass point A in Fig. 6(a) is the closest point to both intersection points B and C . In this case, the midpoint between the first intersection point and the last one is calculated and the mass point is snapped to that midpoint, as point D in Fig. 6(a). However, the first and last cutting points (points S and E) are treated as special “intersection points”. The closest mass points are directly snapped to the first and last cutting points in order to ensure exact starting and ending locations of the cut, as shown in Fig. 6(b).

3.2 Inside Cut Node Snapping

When cutting into a discrete mass spring model, the tip of the cutting tool may reach a location without mass point or spring definition. This problem can be solved by extending node snapping approach from surface models to volumetric models. The objective is to snap some mass points and associated springs onto the cutting planes (as defined earlier in Fig. 3). Fig. 7 shows an illustrative diagram of inside cut snapping. When the cutting tool moves from S_1B_1 to S_4B_4 , surface cut snapping is performed first and mass points S_1 , S_2 , S_3 and S_4 are snapped along the cutting path, as discussed in Section 3.1. Then, inside cut snapping is accomplished by following two steps:

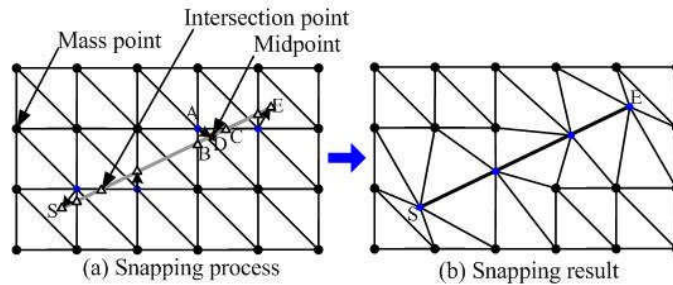


Fig. 6: Special surface cut point snapping cases.

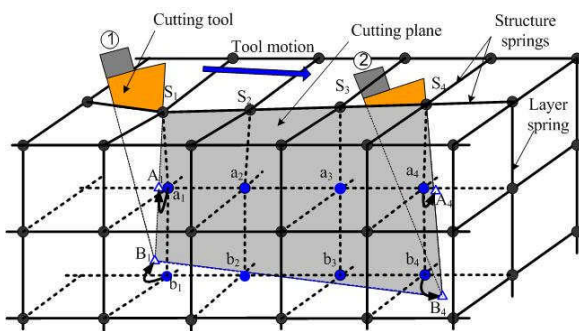


Fig. 7: Inside cut point snapping.

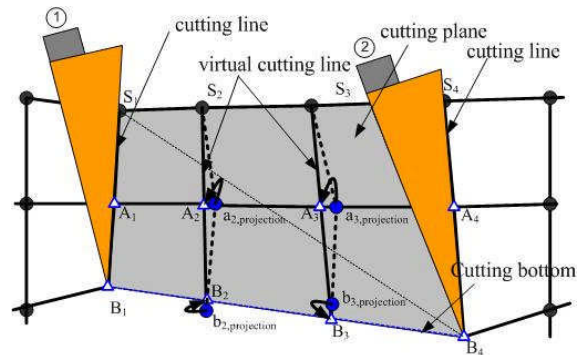


Fig. 8: Inside cut snapping onto the cutting plane.

- (1) Mass points are first snapped onto each cutting line, e.g. S_1B_1 and S_4B_4 in Fig. 7. Mass points b_1 and b_4 are snapped to the bottom cut points B_1 and B_4 . If there are mass points between surface cut points and bottom cut points such as a_1 between S_1 and b_1 , these mass points are projected onto the cutting lines as projection points like A_1 .
- (2) It is possible that some mass points may exist between cutting lines such as mass points a_2 , a_3 , b_2 and b_3 in Fig. 7. These mass points and the associated springs are also projected onto the cutting planes, such as $a_{2,projection}$ and $b_{2,projection}$ in Fig. 8. First, the intersection points between the cutting bottom (e.g. B_1B_4) and the projected springs are calculated. The closest mass points are snapped to the intersection points, such as B_2 and B_3 . This can make sure that some springs are aligned along the cutting bottom. The intersection points (e.g. B_2) and their corresponding surface snapped points (e.g. S_2) are connected to form the “virtual” cutting lines such as S_2B_2 . “Virtual” cutting lines are not the real sampling locations of the cutting tool. At last, other projected mass points on the cutting planes are projected again onto the “virtual” cutting lines. For instance, $a_{2,projection}$ is projected on the “virtual” cutting line S_2B_2 at A_2 , as shown in Fig. 8.

So far the snapping method only deals with the snapping case in one soft tissue. If more than one tissue layers are involved in one cut, the mass point snapping is quite different and more complex, which will be discussed later in section 3.4.

3.3 Open Surface Node Modification

After some mass points and springs are snapped on the cutting planes, the cut is generated by dividing the model along the cutting planes. First, snapped mass points except for the starting and ending points of the cut, are duplicated twice and directly displaced at two sides of the cutting planes such as mass points S_{i1} and S_{i2} for S_i in Fig. 9(b). In our model, the mass of each mass point is represented by mass density [13]. The mass point duplication and

where α_i is the initial surface tension ($0.0 \leq \alpha_i \leq 1.0$); d_i is the cutting depth; h_i is the depth of the mass point i from the model surface; c is a user-defined scaling parameter to control the cut width. For mass points on the model surface, h_i is zero so that w_i has the maximal value as $w_{s,i}$ in Fig. 10. At the cutting bottom, h_i is equal to d_i so that w_i becomes zero. It remains an open question in Biomechanics to determine the initial skin surface tension [12]. Generally, larger α_i means higher surface tension and wider cut open. On the other hand, the cut width cannot be unlimitedly large, which can be easily observed in the real soft tissue incision. A threshold value w_{\max} is applied to limit the width of cut. In general, w_{\max} is slightly smaller than the average of spring length. Equation (2) is then modified as following,

$$w_i = \min\left(c \frac{d_i - h_i}{1 - \alpha_i}, w_{\max}\right) \quad (3)$$

The displacement of duplicated mass points can be calculated by following equations,

$$\begin{aligned} \vec{S}_{i1} &= \frac{w_i}{2} \frac{\vec{n}_i \times \vec{SS}_i}{|\vec{n}_i \times \vec{SS}_i|} \\ \vec{S}_{i2} &= -\frac{w_i}{2} \frac{\vec{n}_i \times \vec{SS}_i}{|\vec{n}_i \times \vec{SS}_i|} \end{aligned} \quad (4)$$

And new positions of duplicated mass points can be calculated by Equation (5),

$$\begin{aligned} S_{i1} &= S_i + \min\left(c \frac{d_i - h_i}{(1 - \alpha_i)}, w_{\max}\right) \frac{\vec{n}_i \times \vec{SS}_i}{|\vec{n}_i \times \vec{SS}_i|} \\ S_{i2} &= S_i - \min\left(c \frac{d_i - h_i}{(1 - \alpha_i)}, w_{\max}\right) \frac{\vec{n}_i \times \vec{SS}_i}{|\vec{n}_i \times \vec{SS}_i|} \end{aligned} \quad (5)$$

Although this cut opening method does not follow the physical law, the generated cut is unconditionally smooth. The cut result is visually smoother than the traditional zig-zag cut edge shown in earlier work [4, 8, 9]. Further more, this method is more efficient in computation than the physically-based numerical integration methods where the cut is generated by the spring forces of disconnected springs.

3.4 Internal Triangle Generation

After the cut is opened by the method in Section 3.3, internal triangles at both sides of the cut are generated to form watertight surfaces for the deformable model. Different from groove generation algorithms of previous work that were applied to homogeneous surface models, the proposed internal triangle generation method for heterogeneous volumetric deformable models features representing different soft tissues layers explicitly at the cutting site. Fig. 11 shows an illustrative diagram of internal triangle generation when the cutting tool cuts from position 1 to position 2 at one tool movement. The model is separated along the cutting plane (A-A plane) to show the inside details in Fig. 12. The internal triangle generation method has following two cases as shown in Fig. 12.

Case 1: only one tissue is cut when the cutting tool moves from S_1B_1 to S_5B_5 as shown in Fig. 12(a). The cut is not deep enough to reach the second tissue layer (Tissue 2). For heterogeneous models, the node snapping is different near the interface between two soft tissues. It is possible that the cutting tool is very close to the interface surface but hasn't reached the interface yet. The closest mass point on the interface is not snapped to the bottom cut point. In Fig. 12(a), although mass point K_5 is closer to B_5 than other mass points, it is not snapped to B_5 . Otherwise, it would indicate that the cutting tool has reached the interface surface. After the inside cut snapping, the cut is opened as discussed in Section 3.3. New internal triangles need to be generated at both sides of the cut. In Case 1, internal triangles are generated between cutting lines and virtual cutting lines as shown in Fig. 12(a). For example, new triangles are generated by the vertex sequence of $S_1B_1S_2$ and $S_2B_1B_2$. Only one side of the cut is shown in Fig. 12(a) and triangles are also generated similarly at the other side of the cut.

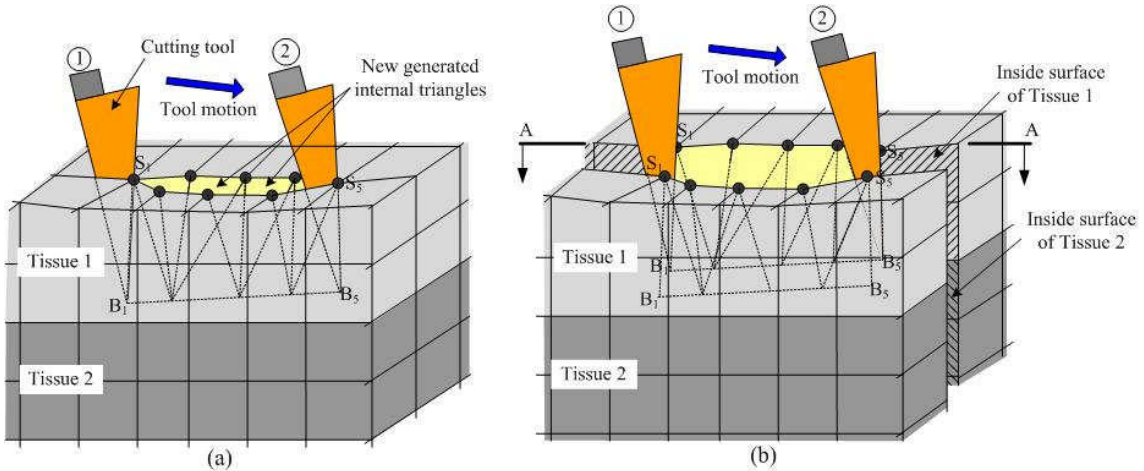


Fig. 11: Cutting on heterogeneous model.

Case 2: more than one tissue layers are cut as the cutting tool moves from S_1B_1 to S_5B_5 at one time step as shown in Fig. 12(b). The node snapping is more complicated near the interface of two tissue layers. (1) When the tip of the cutting tool reaches B_3 , it hasn't cut into tissue 2. After that, the cutting tool cuts into tissue 2 and its tip reaches B_4 and B_5 later. In this situation, B_3 is snapped onto the interface surface. (2) When the cutting tool cuts into another soft tissue and no matter how deep it is, a mass point of that soft tissue should be snapped to the tip of the cutting tool to represent the cutting depth. For example, even if the mass point A_4 is closer to B_4 , a mass point of tissue 2 is snapped to B_4 , in order to ensure the correct cutting depth information.

After the mass point snapping, new triangles are generated at two sides of the cut, similar to the method in the first case. Different sets of triangles are separated by the interface surface. More complex cutting cases exist in accordance with various cutting depths such as the example shown in Fig. 12(c). These complex cases can be considered as the combinations of the two cases we have discussed. The material properties are assigned to these new generated internal triangles according to their vertices' properties. We argue that vertices of a triangle, except for vertices on the model surface or an interface surface, belong to only one type of tissue in our deformable models. For example in Fig. 12(b), Triangle $S_1B_1S_2$ belongs to Tissue 1 because B_1 is mass point of tissue 1 and S_1 and S_2 is on the model surface. Triangle $B_3B_4A_4$ belongs to Tissue 2, since B_3 and B_4 are mass points of tissue 2 and A_4 is on the interface surface. Although the node snapping approach for topological modification does not increase the number of mesh elements, degeneracy such as smaller element size or badly-shaped elements may still occur after the node snapping. Degeneracy can cause system instability of downstream numerical integration for the deformation simulation. A quasi-static algorithm has been developed to implement mesh refinement in our previous work [18]. Mass points are iteratively relocated based on their spring forces.

4. IMPLEMENTATION AND RESULTS

The proposed cutting techniques are implemented on a 2.4 GHz dual-CPU workstation with 2 GB memory and a high-end graphics card. Microsoft® Visual C++6.0 and Open GL® library are the fundamental development tools. The system is integrated with a 6-DOF (degree of freedom) Phantom® desktop, which can provide 3-DOF force feedback. The integration of haptic devices into virtual systems has been discussed in our previous work [16, 17]. Fig. 13(a) shows the system setup for cutting simulation. During the cutting process, topology of the deformable model is modified. In the mean time, the model is deformed by the cutting tool. Numerical integration of the simulation system is based on constrained local static integration method in our previous work [13]. Each mass point is iteratively moved under its spring force but constrained within the bounding box defined by its neighboring mass points. Fig. 13(b) shows an example of cutting a heterogeneous deformable model consisting of a total of 4,152 mass points by using a virtual cutting tool.

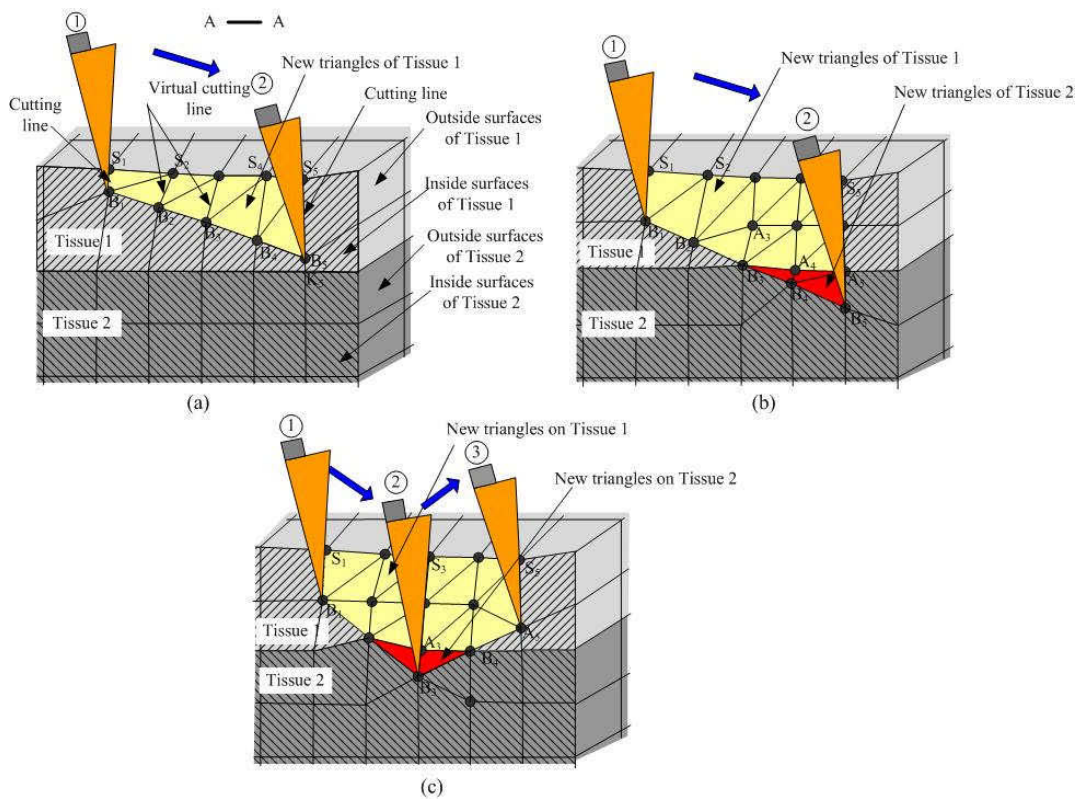
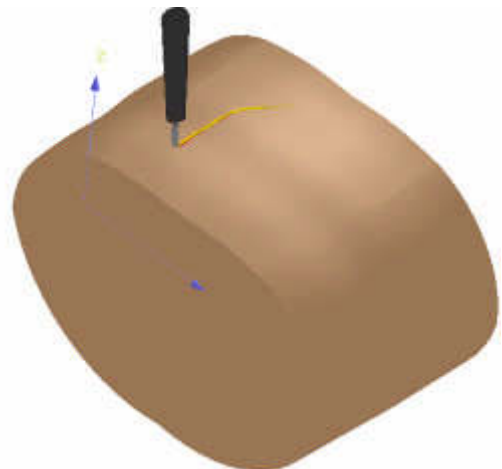


Fig. 12: Cutting cases on the heterogeneous model.



(a) Lab setup with haptic force-feedback interface



(b) Cutting simulation using a surgical scalpel

Fig. 13: Cutting simulation using a Phantom haptic device.

Fig. 14 shows a cut opening result on the model surface. New springs are generated and connected to their neighboring mass points, as shown in the lower right figure. Internal triangles are generated to form a watertight surface as shown in the lower left figure. The cut is smooth as shown in Fig. 14.

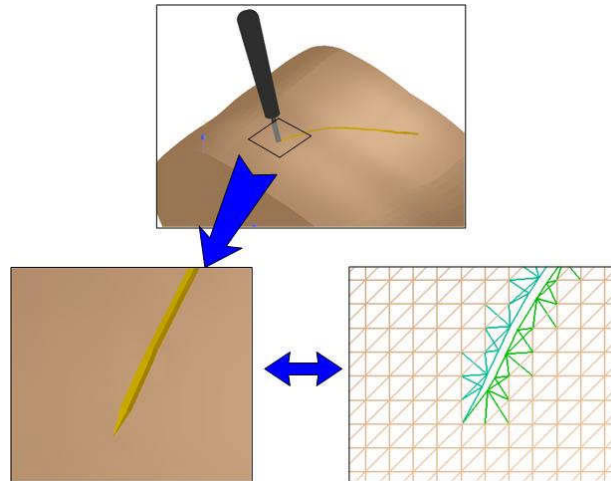


Fig. 14: Arbitrary cutting result and new generated springs at cutting site.

Fig. 15 shows the heterogeneity of the deformable model at the cutting site. Fat tissues and muscles are represented by different colors. Thickness of each tissue layer depends on geometry of the deformable model. The cutting result on heterogeneous model is able to provide users with most important visual feedback such as color or texture. On the other hand, heterogeneous material properties like stiffness on each layer also gives the user appropriate tactile cue. With realistic visual and haptic feedback, users can easily control their cutting behaviors during the cutting.

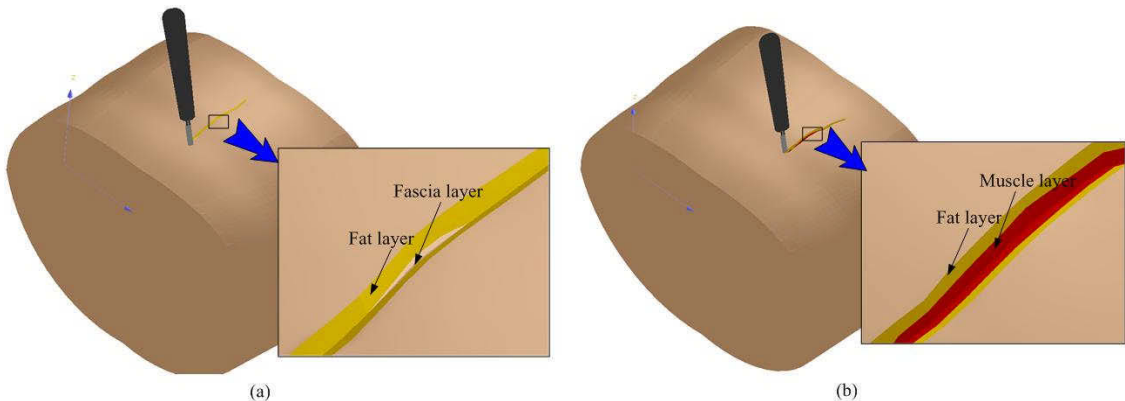


Fig. 15: Multiple layers at different cutting sites: (a) cutting into right rectus, (b) cutting into linea alba.

Fig. 16 shows the process of cutting soft tissues on a heterogeneous leg model to expose the bone (tibia). Skin and part of fascia are cut open first, as shown in Fig. 16(a). Then the model is cut deeper inside until the tibia is reached. Because bones are considered as rigid objects, they are not cut open by a general cutting tool like a scalpel. Users can see the intact bone surfaces and perform further surgery on bones.

Fig. 17 shows an example of continuous cuts on a human leg model. After the model is cut first as shown in Fig. 17(b), new cut can be done on the existing cut either to deepen or to lengthen the cut. Fig. 17(c) shows an example of making the old cut deeper. As a result, the muscle layer is exposed by the second cut. The cut is further deepened as shown in Fig. 17(d). This provides users the training scenario of cutting the soft tissues layer by layer as the surgeons do in real surgery.

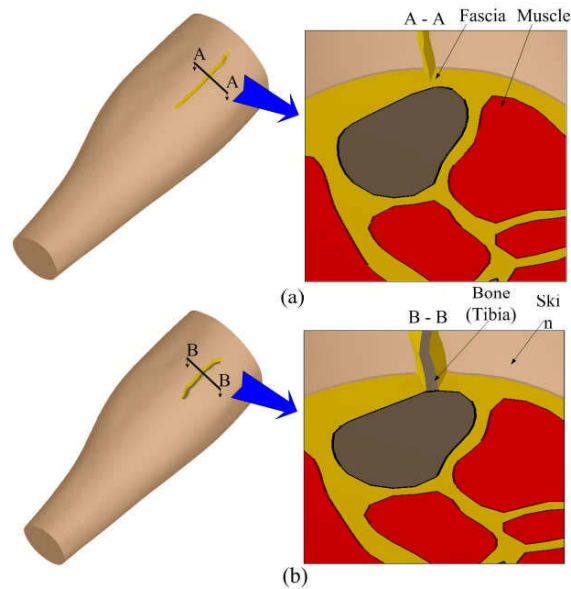


Fig. 16: Cutting results on different cutting depths.

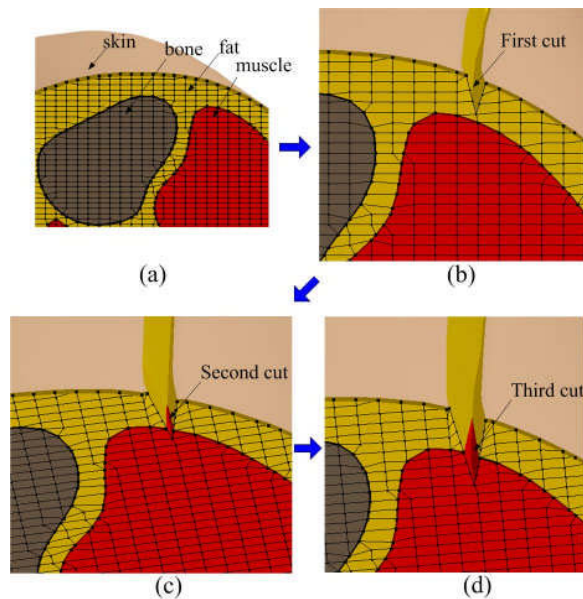


Fig. 17: The detailed results of continuous cuts on a leg model. (a) original model; (b) cutting result after the first cut; (c) cutting result after the second cut; (d) cutting result after the third cut.

5. CONCLUSION

In this paper, cutting techniques are proposed for cutting simulation on volumetric heterogeneous deformable models. 3D node snapping and topology modification approaches are presented to generate the smooth cut. The cut can present heterogeneous interior structures and material properties of deformable models. The proposed cutting techniques can enhance the fidelity and realism of surgical simulation. They can also be used to other virtual simulation systems when topological modification is involved.

6. ACKNOWLEDGEMENT

This work was partially supported by the National Science Foundation (NSF) Grant (DMI-0300297, CMMI-0553310, CMMI-0800811) and the Army Research Office (Grant #W911NF-04-D-0003) to North Carolina State University. Their support is greatly appreciated.

7. REFERENCES

- [1] Mosegaard, J.: Realtime cardiac surgery simulation, PhD Dissertation, Aarhus University Hospital, Denmark, 2004.
- [2] Fuller, J. R., Surgical technology principles and practice, second edition, W. B. Saunders Company, 1986.
- [3] Bruyns, C. D.; Senger, S.; Menon, A.; Montgomery, K.; Wildermuth, S.; Boyle, R.: A survey of interactive mesh-cutting techniques and a new method for implementation generalized interactive mesh cutting using virtual tools, *Journal of Visualization and Computer Animation*, 13, 2002, 21-42.
- [4] Bro-nielsen, M.; Helfrick, D.; Glass, B.; Zeng, X.; Connacher, H.: VR simulation of abdominal trauma surgery, *Proceedings of Medicine Meets Virtual Reality 6*, San Diego, California, January 28-31, 1998, 117-123.
- [5] Bielser, D.; Maiwald, V. A.; Gross, M. H.: Interactive cuts through 3-Dimensional Soft Tissue, *Computer Graphics Forum (Eurographics 99 Proc.)* 18(3), 1999, 31-38.
- [6] Lim, Y.-J. De, S.: On the use of mesh-free methods and a geometry based surgical cutting algorithm in multimodal medical simulations, *Proceedings of the 12th International Symposium on Haptic Interfaces for Virtual Environment and Teleoperator Systems (HAPTICS'04)*, 2004, 295-301.
- [7] Zhang, H.; Payandeh, S.; Dill, J.: On cutting and dissection of virtual deformable objects, *Proceedings of the 2004 IEEE International Conference on Robotics & Automation*, April 2004, 3908-3913.
- [8] Nienhuys, H.-W.; van der Stappen, A.F.: A surgery simulation supporting cuts and finite element deformation, *Proceedings Medical Image Computing and Computer Assisted Intervention (MICCAI)*, 2001, 145-152.
- [9] Delingette, H.; Cotin, S.; Ayache, N.: A hybrid elastic model allowing real-time cutting, deformations and force-feedback for surgery training and simulation, *Proceeding computer animation* 1999, 70-81.
- [10] Lin, S.; Lee, Y.-S.; Narayan, R.; Shin, H.: Bio-Tissues Modeling and Interface Development for Bio-Manufacturing and Medical Applications, *Proceedings of the 2007 Industrial Engineering Research (IERC) Conference*, Nashville, TN, May 19-23 2007, 281-286.
- [11] Lin, S.; Lee, Y.-S.; Narayan, R.: Heterogeneous Soft Material Modeling and Virtual Prototyping with 5-DOF Haptic Force Feedback for Product Development, *Proceedings of The 3rd International Conference on Advanced Research in Virtual and Rapid Prototyping, (VRAP 2007)*, Leiria, Portugal, September 24-28, 2007, 187-193.
- [12] Fung, Y. C.: *Biomechanics: mechanical properties of living tissues*, second Edition, Springer-Verlag, New York, 1993.
- [13] Lin, S.; Lee, Y.-S.; Narayan, R.: Snapping Algorithm and Heterogeneous Bio-Tissues Modeling for Medical Surgical Simulation and Product Prototyping, *Virtual and Physical Prototyping*, 2(2), 2007, 89-101.
- [14] Mollemans, W.; Schutyser, F.; Cleynebreugel, J. V.; Suetens, P.: Tetrahedral mass spring model for fast soft tissue deformation, *Proceedings of Surgery Simulation and Soft Tissue Modeling: International Symposium, IS4TM*, 2003, 145-154.
- [15] Meier, U.; Lopez, O.; Monserrat, C.; Juan, M.C.; Alcaniz, M.: Real-time deformable models for surgery simulation: a survey, *Computer Methods and Programs in Biomedicine*, 77, 2005, 183-197.
- [16] Lin, S.; Lee, Y.-S.; Narayan, R.: Heterogeneous Material Modeling and Virtual Prototyping with 5-DOF Haptic Force Feedback for Product Development, (in print), Accepted for publication in *International Journal of Mechatronics and Manufacturing Systems*, 2007.
- [17] Lin, S.; Lee, Y.-S.; Narayan, R.: Collaborative Haptic Interfaces and Distributed Control for Product Development and Virtual Prototyping, *Proceedings of 2007 International Manufacturing Science & Engineering Conference*, Atlanta, GA, USA, October 15-18, 2007.
- [18] Lin, S.; Lee, Y.-S.; Narayan, R.: Topology Modification and Mesh Relaxation for Medical Surgical Cutting on Heterogeneous Deformable Tissues, (under review), Submitted to *Computer Aided Design*, 2008.